RSC Advances

ROYAL SOCIETY OF CHEMISTRY

www.rsc.org/advances

RSC Advances

ARTICLE

Fused π-Conjugated Imidazolium Liquid Crystals: Synthesis, Self-Organization, and Fluorescent Properties

Received 00th January 20xx,
Accepted 00th January 20xx

DOI: 10.1039/x0xx00000x

www.rsc.org/

Koji Takagi,*[a] Koji Yamauchi,[a] Seiko Kubota,[a] Shusaku Nagano,[b] Mitsuo Hara,[b] Takahiro Seki,[b] Kazuya Murakami,[c] Yousuke Ooyama,[c] Joji Ohshita,[c] Masaharu Kondo,[a] and Hyuma Masu[d]

Fused π-conjugated imidazolium compounds bearing two or three long alkoxy chains and various counter anions were systematically prepared following to our reported synthetic route. On the basis of DSC measurements and POM observations, the combination of three alkoxy chains longer than the dodecyl group and moderately coordinating anions was important to obtain an enatiotropic mesophase. VT-XRD measurements coupled with a single crystal X-ray structure of model compound revealed a hexagonal columnar structure supported by ionic interactions. The regularity of self-organized nanostructure was governed by the alkoxy chain length and the coordinating ability of counter anion. In solution state, UV-vis and fluorescence peak maxima were influenced by the number of alkoxy chains and independent upon the chain length and anion character. On the contrary, the alkoxy chain length and the coordinating ability of counter anion had a large impact on the fluorescence spectra in solid state. A longer wavelength emission at around 560 nm was observed for compounds with the highly regular hexagonal columnar structure. From the result of fluorescence lifetime measurements, the interaction between fused π-conjugated imidazolium cations was suggested.

Introduction

Thermotropic liquid crystals with well-defined self-organized nanostructures have been attracting much attention in the field of materials science. Among many thermotropic liquid crystals, columnar liquid crystals are of particular interest because the one-dimensional self-organization of liquid crystalline molecules enables anisotropic and efficient energy, ion, and charge transports along the column axis.[1] The discovery of columnar liquid crystalline phase therefore opened up a new research area in the potential application for optoelectronic devices.[2]

The self-organization of liquid crystalline molecules is commonly supported by non-covalent interactions including π-π stacking, hydrogen bonding, and van der Waals force. On the other hand, ionic interactions are relatively strong to realize a long-range columnar self- organization with the higher order structure in large area. Accordingly, considerable attention has been devoted to the synthesis and characterization of ionic liquid crystals, which merges the intrinsic feature of ionic liquids (low melting temperature, non-volatile, and non-flammable) with that of liquid crystals (self-organization, orientation anisotropy, and phase transition). In early times, amphiphilic molecules comprising small *N*-alkylammonium, *N*-alkylpyridinium, and *N*,*N*′-dialkylimidazolium units were synthesized to demonstrate the influence of alkyl chain length and counter anion on the liquid crystalline behavior.[3] This simple molecular design utilizing imidazolium units as a polar group (Fig. 1, Type A) gave task-specific smart functional materials. Kato et al have succeeded in one and two dimensional ion transports by optimizing a chemical structure of liquid crystalline molecules, which revealed a potential utility as electrolytes for batteries and capacitors.[4] Douce et al have shown the use of an imidazolium-based ionic liquid crystal as a template to synthesize silver and gold nanoparticles.[5] On the other hand, Fukushima and Aida et al have synthesized a triphenylene-based liquid crystal with paraffinic alkyl chains whose termini are decorated with the imidazolium ion group.[6] Müllen et al have prepared imidazolium-based amphiphilic hexa-*peri*-hexabenzocoronenes with two hydrophobic long alkyl chains and two hydrophilic group consisting of alkyl chains terminated with ionic imidazolium group.[7] These materials demonstrated a stable columnar phase of discotic liquid crystal and a self-assembled nanofiber formation on solid substrates. The molecular design used for synthesizing these molecules (Fig. 1, Type B) is different from the conventional approach. Recently, new class of ionic liquid crystals comprising heteroatom-containing π-conjugated segments (imidazolium and phosphonium) have been reported (Fig. 1, Type C).[8,9] The molecular structure is resemble to that in Type A, however, an extended π-conjugated system offers

[a] Department of Materials Science and Engineering, Graduate School of Engineering, Nagoya Institute of Technology, Gokiso-cho, Showa-ku, Nagoya, Aichi 466-8555 (Japan) *takagi.koji@nitech.ac.jp (Koji Takagi)
[b] Department of Molecular Design and Engineering, Graduate School of Engineering, Nagoya University, Furo-cho, Chikusa-ku, Nagoya, Aichi 464-8603 (Japan)
[c] Department of Applied Chemistry, Graduate School of Engineering, Hiroshima University, 1-3-2 Kagamiyama, Higashi-Hiroshima, Hiroshima 739-8527 (Japan)
[d] Center for Analytical Instrumentation, Chiba University, 1-33 Yayoi-cho, Inage-ku, Chiba, Chiba 263-8522 (Japan)

† Electronic Supplementary Information (ESI) available: The synthesis and characterization details. NMR spectra, DSC thermograms, POM images, XRD profiles, single crystal X-ray structure, and optical properties. CCDC 1437162. For ESI and crystallographic data in CIF format. See DOI: 10.1039/x0xx00000x

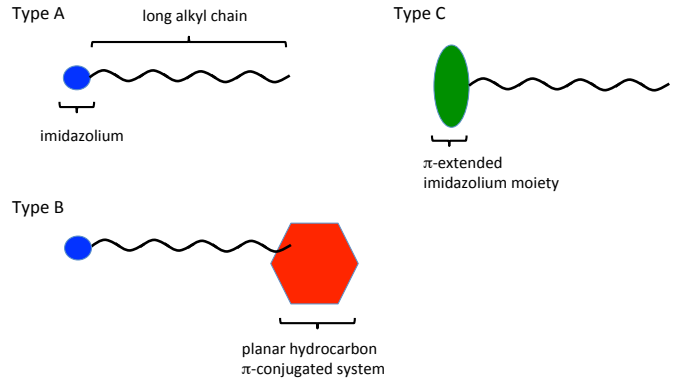

Fig. 1 Molecular design of imidazolium-based liquid crystals.

intriguing properties, such as phase tunability, multiphoton excitation, gelation of organic solvents, and reversible mechano(fluoro)chromism.

We have recently developed novel fused π-conjugated (benz)imidazolium compounds. The successive intramolecular cyclization utilizing the nucleophilic attack by two imidazole nitrogen atoms enabled the construction of a rigid molecular framework containing π-extended imidazolium units.[10] In addition, the optical properties of these compounds (absorption and emission wavelengths, fluorescence quantum yield, and solvatofluorochromism) could be controlled by introducing electron-donating and accepting substituents on the benzene ring at the 2-position of (benz)imidazole or by changing counter anions.[11] These findings indicate that fused π-conjugated imidazolium compounds are fascinating candidates not only for fundamental studies but also for potential light-emitting materials. However, observed optical properties are restricted to those in solution state. As a part of our ongoing research about imidazole-based π-conjugated systems, we have conceived the synthesis and characterization of fused π-conjugated imidazolium liquid crystals that harnesses a rigid fluorescent π-conjugated imidazolium core with a non-ionic flexible alkoxyphenyl moiety (Fig. 2). The influence of alkoxy chain (number and length) and counter anion on the self-organization and fluorescent properties were revealed by differential scanning calorimetry (DSC), polarized optical

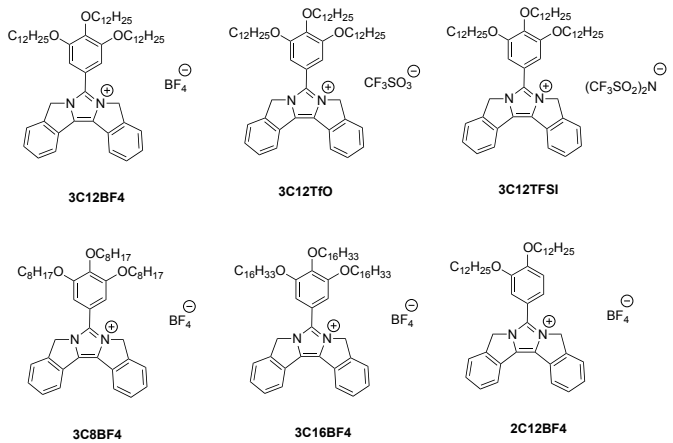

Fig. 2 List of fused π-conjugated imidazolium compounds.

microscopy (POM), variable temperature X-ray diffraction (VT-XRD), ultraviolet-visible (UV-vis) absorption and fluorescence emission spectroscopies, and fluorescence lifetime measurement.

Experimental

Materials and instruments used for this work are described in Electronic supplementary information (ESI†).

Synthesis

Fused π-conjugated imidazolium compounds bearing di- and trialkoxyphenyl group at the 2-position of imidazole were synthesized according to a manner we have reported previously.[11] Typical procedures for preparing **3C12BF4** with a 3,4,5-tridodecyloxyphenyl group and a tetrafluoroborate anion are as follows:

4,5-Bis(2'-(hydroxymethyl)phenyl)-2-(3",4",5"-tridecyloxyphenyl)imidazole (imidazole ring formation)

A mixture of 1,2-bis(2'-(*t*-butyldimethylsiloxymethyl)phenyl)ethane-1,2-dione (0.50 g, 1.0 mmol), 3,4,5-tridodecyloxybenzaldehyde (0.99 g, 1.5 mmol), L-proline (18 mg, 0.15 mmol), and ammonium acetate (3.0 g, 39 mmol) in EtOH (4 mL) and 1,4-dioxane (2 mL) was heated at 90 °C for 24 h. Water was added and an aqueous phase was extracted with CH_2Cl_2. The combined organic phase was rinsed with brine and dried over $MgSO_4$. The solvent was removed and the remaining brown solid was dissolved in a mixture of THF (95 mL), TBAF solution in THF (1 M, 4.5 mL), and AcOH (0.26 mL) to stir at room temperature overnight. The solvent was removed and dissolved in CH_2Cl_2 that was rinsed with sat. aqueous $NaHCO_3$ and dried over $MgSO_4$. The solvent was removed and the crude product was purified by SiO_2 column chromatography (hexane : ethyl acetate = 8 : 3, Rf = 0.40) to obtain a yellow solid (0.53 g, 59% yield). ^{1}H-NMR ($CDCl_3$) δ ppm 0.79–0.98 (9H), 1.26 (48H), 1.47 (6H), 1.77 (6H), 4.00 (6H), 4.59 (brs, 2H), 4.75 (brs, 2H), 7.04 (s, 2H), 7.10 (brs, 2H), 7.21 (brs, 2H), 7.26–7.37 (2H), 7.45 (brs, 2H), 11.68 (brs, 1H).

1,3-Dihydro-4,5-bis(2'-(chloromethyl)phenyl)-2-(3",4",5"-tridodecyloxyphenyl)imidazolium chloride (chlorination)

To a solution of 4,5-bis(2'-(hydroxymethyl)phenyl)-2-(3",4",5"-tridecyloxyphenyl)imidazole (0.53 g, 0.59 mmol) in CH_3CN (36 mL) and CH_2Cl_2 (28 mL) was added $SOCl_2$ (0.42 mL, 5.9 mmol), and the mixture was stirred overnight at room temperature. After the solvent was removed, a greenish brown solid was obtained quantitatively which was directly used for the next reaction. ^{1}H-NMR ($CDCl_3$) δ ppm 0.86 (9H), 1.24 (54H), 1.77 (6H), 4.03 (6H), 4.60 (4H), 6.83 (6H), 7.00 (brs, 2H), 7.40 (brs, 2H), 14.25 (brs, 2H).

Fused imidazolium chloride with three dodecyloxy chains (3C12Cl) (intramolecular cyclization)

To a solution of 1,3-dihydro-4,5-bis(2'-(chloromethyl)phenyl)-2-(3",4",5"-tridodecyloxyphenyl)imidazolium chloride (0.58 g, 0.59 mmol) in DMF (68 mL) was added LiHMDS solution in THF (1 M, 1.2 mL) at 0 °C, and the mixture was stirred overnight at room temperature. After the solvent was removed, water and $CHCl_3$ were added in the separating funnel. An aqueous phase was extracted with $CHCl_3$. The combined organic phase was rinsed with brine and dried over $MgSO_4$. The solvent was removed and the remaining

solid was dissolved in $CHCl_3$ (30 mL) to be heated to 60 °C for 6 h. After the solvent was removed, the remaining solid was dissolved in $CHCl_3$ to be poured in ethyl acetate to obtain a colorless solid (0.24 g, 44% yield). ^{1}H-NMR ($CDCl_3$) δ ppm 0.84–0.92 (9H), 1.21–1.41 (48H), 1.46–1.57 (6H), 1.73–1.89 (6H), 4.08 (t, *J* = 6.48 Hz, 2H), 4.23 (t, *J* = 6.11 Hz, 4H), 5.89 (s, 4H), 7.45–7.51 (m, 4H), 7.52–7.58 (m, 2H), 7.67 (d, *J* = 7.58 Hz, 2H), 7.84 (d, *J* = 7.58 Hz, 2H).

Fused imidazolium tetrafluoroborate with three dodecyloxy chains (3C12BF4) (anion exchange)

To a solution of **3C12Cl** (50 mg, 55 mmol) in $CHCl_3$ (2 mL) was added $Et_3O{\cdot}BF_4$ solution in CH_2Cl_2 (1 M, 66 mL), and the mixture was stirred at room temperature for 24 h. After water was added, an aqueous phase was extracted with CH_2Cl_2. The combined organic phase was washed with water and dried over $MgSO_4$. The solvent was removed to obtain a colorless solid (42 mg, 80% yield). m.p. 187.7–189.6 °C. Anal Calcd for $C_{59}H_{89}BF_4N_2O_3$: C 73.73, H 9.33, N 2.91 %; Found: C 73.70, H 9.50, N 2.89 %. ^{1}H-NMR ($CDCl_3$) δ ppm 0.84–0.94 (9H), 1.21–1.41 (48H), 1.46–1.57 (6H), 1.73–1.89 (6H), 4.05 (t, *J* = 6.60 Hz, 2H), 4.10 (t, *J* = 6.24 Hz, 4H), 5.48 (s, 4H), 7.08 (s, 2H), 7.39–7.44 (m, 2H), 7.44–7.50 (m, 2H), 7.61 (d, *J* = 7.34 Hz, 2H), 7.73 (d, J = 7.58 Hz, 2H). ^{13}C-NMR ($CDCl_3$) δ ppm 14.14, 22.73, 26.15, 26.29, 29.40, 29.45, 29.69, 29.76, 29.78, 29.83, 30.49, 31.99, 52.89, 69.84, 73.63, 105.31, 115.67, 120.66, 123.56, 126.00, 128.57, 129.03, 137.92, 138.99, 141.48, 154.16.

Results and discussion

Synthesis

Four fused π-conjugated imidazolium chlorides bearing di- and trialkoxyphenyl group at the 2-position of imidazole were synthesized from 1,2-bis(2'-(*t*-butyldimethylsiloxymethyl)phenyl)ethane-1,2-dione[11] in three steps (Scheme 1). In the last step, the heating of $CHCl_3$ solution was necessary to complete the intramolecular double cyclization by overcoming the steric hindrance of the phenyl group at the 2-position of imidazole. These compounds were found to be thermally unstable and decomposed upon heating over clearing temperatures (data not shown here). This is probably due to the nucleophilic attack of the chloride anion toward the methylene carbon at the bridge position, which hampered the in-depth characterization of the liquid crystalline behavior. We therefore performed the anion exchange reaction from chloride to weakly coordinating tetrafluoroborate (BF_4^-), trifluoromethanesulfonate (TfO^-), and bis(trifluoromethanesulfonyl)imidate ($TFSI^-$). $Et_3O{\cdot}BF_4$ was used for the anion metathesis from chloride to tetrafluoroborate following to the Bielawski's protocol.[8c] The anion metatheses from chloride to trifluoromethanesulfonate and bis(trifluoromethanesulfonyl)imidate were performed using the metal salt of corresponding anions. To understand the prerequisite chemical structure for obtaining ionic liquid crystals, a reference compound without the fused structure (**3C12BF4ref**) was also prepared (See ESI† for the chemical structure). The structure and

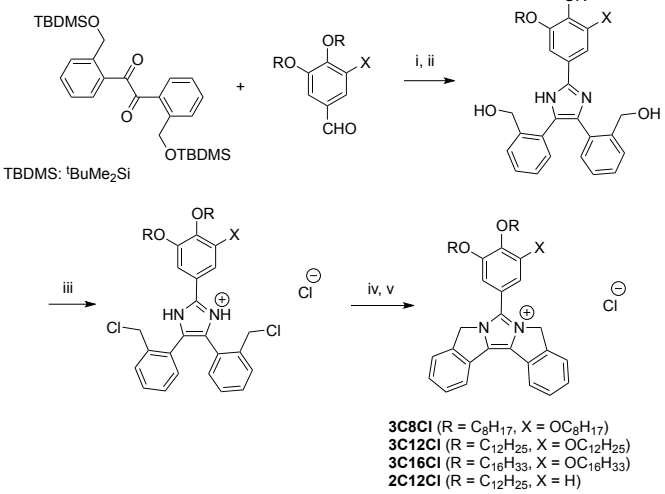

Scheme 1 Synthetic route to fused π-conjugated imidazolium chlorides. (i) L-proline, NH_4OAc, DOX, EtOH, 90 °C, 24 h, (ii) TBAF in THF (1 M), AcOH, THF, rt, 24 h, (iii) $SOCl_2$, MeCN, CH_2Cl_2, rt, overnight, (iv) LiHMDS in THF (1 M), DMF, rt, overnight, (v) $CHCl_3$, 60 °C, 6 h.

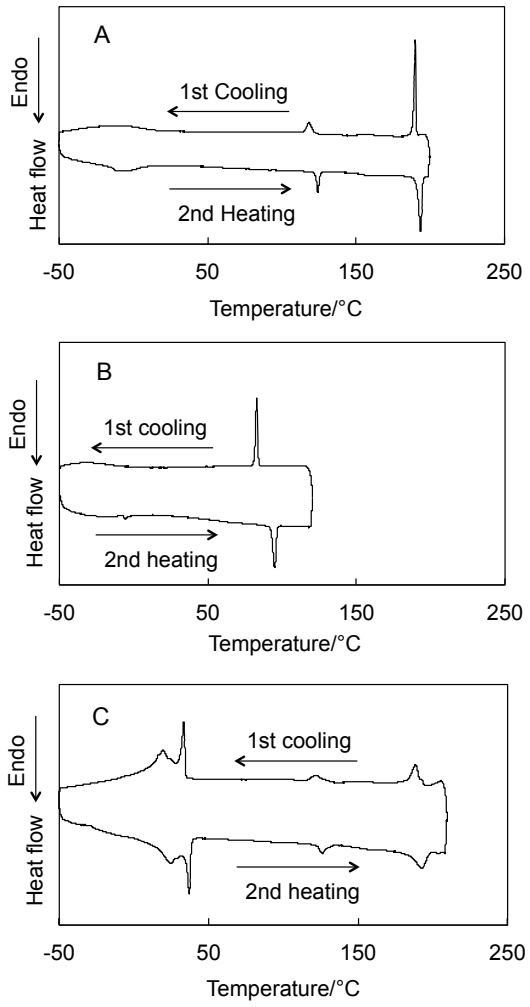

Fig.3 DSC thermograms of (A) **3C12BF4**, (B) **3C12OTf**, and (C) **3C16BF4** in first cooling and second heating processes at 5 °C/min.

purity of all final compounds were fully identified by NMR spectra and elemental analyses (ESI†).

DSC measurement

Thermal properties of six fused π-conjugated imidazolium compounds (Fig. 2) were investigated by DSC measurements under the nitrogen flow. As indicated in Fig. 3, the phase transition behavior was significantly influenced by both the alkoxy chain length and counter anion. As for **3C12BF4** having the middle chain length (Fig. 3A), the crystallization was suppressed in the cooling process and an enantiotropic mesophase having two phase transitions at 124 °C and 158 °C in the heating process was observed between the glass transition temperature at around –10 °C and the clearing temperature at 193 °C (ΔH = 9.61 kJ·mol^{-1}). **3C12OTf** with a trifluoromethanesulfonate anion exhibited a similar but obscure phase transition before going through the clearing temperature (Fig. 3B). A transition temperature to an isotropic phase (95 °C) and an enthalpy change (ΔH = 5.72 kJ·mol^{-1}) were decreased compared with **3C12BF4**, which implies the relatively ill-regulated structure of the mesophase as a consequence of weak cation–anion interaction.[12] On the other hand, **3C16BF4** having the maximum chain length exhibited an enantiotropic mesophase in the wide temperature range (Fig. 3C). Although multiple phase transition peaks with large or small enthalpy changes were observed, the complete characterization of each phase was difficult due to the similar POM images and XRD profiles at different temperatures. Basically, hexagonal columnar phases were confirmed as evidenced by VT-XRD measurements (*vide infra*). In contrast to these three fused π-conjugated imidazolium compounds, **3C8BF4**, **2C12BF4**, and **3C12TFSI** exhibited different phase transition behaviors (Fig. S32–34 in ESI†). **3C8BF4** having the minimum chain length showed only isotropic liquid–crystal transition at 197 °C in the cooling process (Fig. S32). In the heating process, crystal melting and crystal re-growing transitions were observed at 150 °C and 165 °C, respectively. **2C12BF4** bearing two dodecyloxy chains also did not show a mesophase (Fig. S33). Transition enthalpies at the clearing temperature were much larger (23.3 kJ·mol^{-1} and 50.8 kJ·mol^{-1} for **3C8BF4** and **2C12BF4**, respectively) than those of liquid crystalline compounds. In the case of **3C12TFSI** with a bis(trifluoromethanesulfonyl)imidate anion, no phase transition could be observed in the cooling process (Fig. S34) and the supercooling state was kept for several hours. The bulky anion is supposed to interrupt the self-organization of molecules. In addition, any mesophase was not observed for a compound with one octyloxy chain and tetrafluoroborate anion. Therefore the careful molecular design is required for developing a liquid crystalline state of these kinds of molecules. Thermal properties of liquid crystalline compounds are summarized in Table 1 (See also Table S1 in ESI† for thermal properties of other compounds).

Table 1. Phase transition temperatures[a] (°C) and corresponding enthalpies (kJ·mol^{-1}) of ionic liquid crystals.

compound	thermal properties[b]
3C12BF4	G –9.7 (7.03) Col_{hex1} 124.5 (2.79) Col_{hex2} 158.2 (NA[c]) Col_{hex3} 193.3 (9.61) Iso
3C12OTf	G –6.1 (NA[c]) Col_{hex1} 66.6 (NA[c]) Col_{hex2} 94.7 (5.72) Iso
3C16BF4	Col_{hex1} 21.5 (14.7) Col_{hex2} 36.9 (16.6) Col_{hex3} 125.4 (2.34) Col_{hex4} 191.1 (7.86) Iso

[a] Peak temperatures obtained by the DSC measurement in the second heating process at 5 °C/min.
[b] G: glass, Col_{hex}: hexagonal columnar, Iso: isotropic.
[c] Peaks are too weak to accurately calculate values.

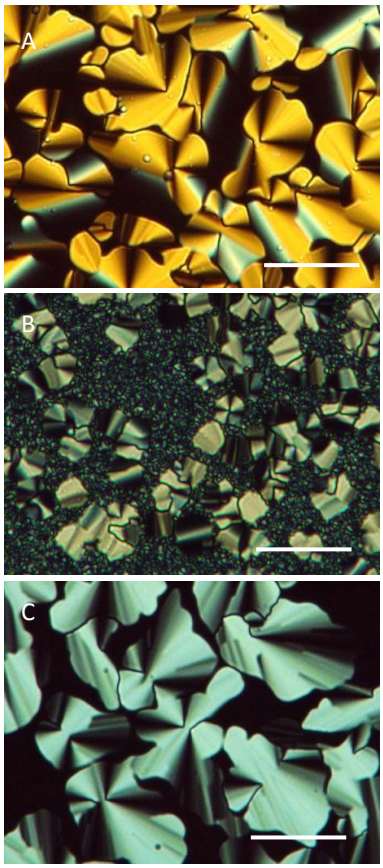

Fig. 4 POM images of (A) **3C12BF4** at 180 °C, (B) **3C12OTf** at 75 °C, and (C) **3C16BF4** at 180 °C. The scale-bars shown in images denote 40μm.

POM observation

The liquid crystalline properties of fused π-conjugated imidazolium compounds were investigated by POM on slowly cooling from the isotropic liquid phase (Fig. 4). As for **3C12BF4**, **3C12OTf**, and **3C16BF4**, the observation of birefringent and fluidic appearance suggested their liquid crystalline nature. The observed focal conic fan-shaped textures with a smooth surface are in consistent with the presence of columnar mesophase. The texture appeared in **3C12OTf** was relatively obscure implying the relatively ill-regulated structure of the mesophase. As we described in the previous section, **3C12TFSI** did not show a birefringence irrespective of the temperature in the cooling process; however, the still standing at 25 °C for 1 day resulted in the observation of a birefringence derived from crystal (Fig. S38 in ESI†).

XRD measurement

To confirm the detailed columnar liquid crystal structures, XRD measurements were performed for all compounds as well as **3C12BF4ref** on cooling from the clearing temperature. A X-ray diffraction pattern of **3C12BF4** in the mesophase at 100 °C had d-spacings of 38.4, 22.1, 19.1, 14.5, and 12.8 Å with the reciprocal ratio of 1 : $3^{1/2}$: 2 : $7^{1/2}$: 3, which correspond to the Miller indexes of (100), (110), (200), (210), and (300), respectively (Fig. 5, red line). This fact unambiguously indicates that **3C12BF4** has a hexagonal columnar (Col_{hex}) structure with a lattice parameter of a = 44.4 Å at this temperature. In addition to a broad halo at around 4.4 Å due to the spacing between alkoxy chains, a peak was observed at 6.3 Å (2theta = 14.0 degree) stemmed from a packing distance (c) of assembled units along the columnar axis.[13] Accordingly, the number of molecules in the unit cell (Z) could be estimated as 6.0 for ρ = 0.9 (Table 2 and Fig. 6). At the higher temperature below 180 °C, **3C12BF4** still maintained a hexagonal columnar structure (Fig. S40 in ESI†). It was found, however, that an inter-columnar distance (a) was decreased with increasing temperature (Table S2 in ESI†). On the other hand, a packing distance along the columnar axis (c) was slightly increased with gradually heating a mesophase and broad peaks in the wide angle region became weak at 180 °C. The smaller a and larger c values at higher temperatures are likely caused by a greater degree of melting of alkoxy chains.

The single crystal X-ray structure analysis was then carried out for **3C1BF4** with methoxy groups instead of long alkoxy chains, which was grown from CH_2Cl_2 and acetone. As shown in Fig. 7 and Fig S47 in ESI†, a tetrafluoroborate anion is located just on top of imidazolium cation. Thus the fused π-conjugated system was slightly bent from the planar structure. Each molecules are stacked in a zigzag fashion to form a columnar structure along the *c* axis with a layer spacing of 7.5 Å that is supported by ionic interactions between imidazolium cation and tetrafluoroborate anion.

3C12OTf also had a hexagonal columnar structure with a = 41.2 Å that is smaller than that of **3C12BF4** (a = 44.4 Å) indicating a tight packing of neighboring columns. Diffraction peaks in the small angle region were broad and a packing distance along the columnar axis (c) could not be clearly observed even at 25 °C (Fig. 5, blue line and Fig. S41 in ESI†). These results are stemmed from the weak ionic interaction between imidazolium cation and trifluoromethanesulfonate anion. In contrast, **3C16BF4** demonstrated sharp and pronounced diffraction peaks correspond to the Miller indexes of (100), (110), (200), (210), and (300) in the wide temperature range (Fig. 5, green line and Fig. S42 in ESI†). Higher order peaks assignable to (220) and (310) reflections were also observed particularly at 70 °C and 150 °C. All these reflections strongly suggest the production of a hexagonal columnar structure. Some reflections between 10 degree and 25 degree were observed,

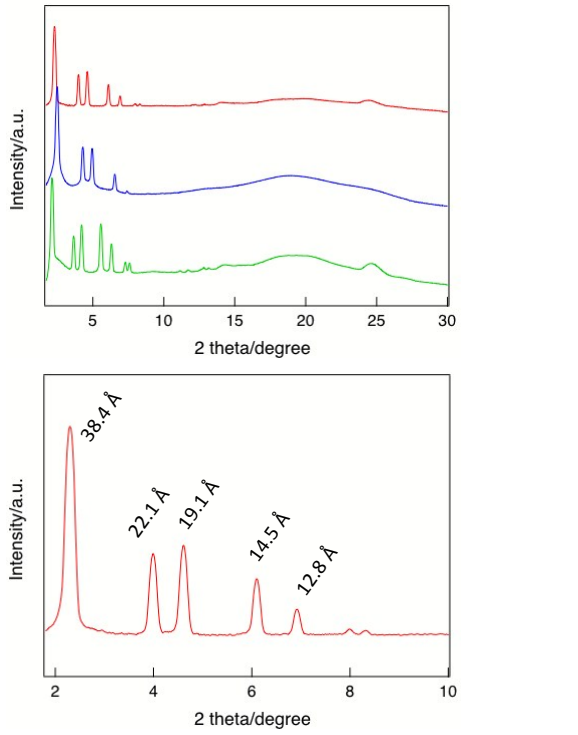

Fig. 5 Top: XRD profiles of (red line) **3C12BF4** at 100 °C, (blue line) **3C12OTf** at 75 °C, and (green line) **3C16BF4** at 70 °C. Bottom: Enlarged XRD profile of **3C12BF4** in the small angle region.

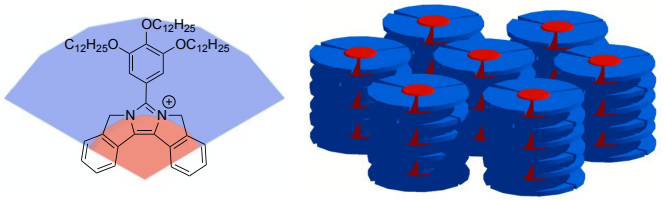

Fig. 6 Schematic illustration of hexagonal columnar structure given by **3C12BF4**.

Table 2. VT-XRD results for Col_{hex} phase of **3C12BF4**.

	Spacing/Å		Miller index	Z
	d_{obs}	d_{calc}		
Col_{hex}	38.4	38.4	100	6.0
a = 44.4 Å	22.1	22.2	110	
c = 6.3 Å	19.1	19.2	200	
T = 100 °C	14.5	14.5	210	
ρ = 0.9	12.8	12.8	300	
M = 961.15	11.1	11.1	220	
	10.6	10.7	310	
	6.3	NA	001	

a and c: cell parameter, T: temperature, ρ: density, M: molecular weight, Z: number of molecules in an unit cell, d_{obs} and d_{calc}: observed and calculated layer spacing.

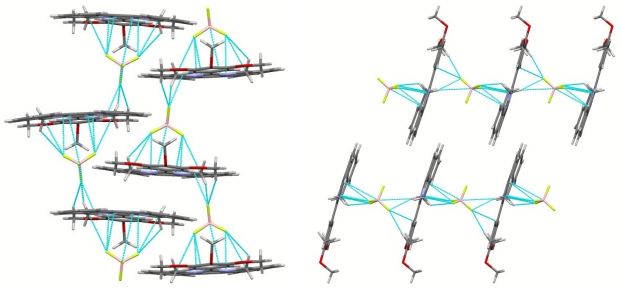

Fig. 7 Packing structure of **3C1BF4** (model compound) viewed from (left) *a* axis and (right) *b* axis. The short contacts within van der Waals radii are indicated by sky blue lines.

however, these small peaks mostly ascribed to the intermolecular interaction are difficult to be precisely assigned at the present stage. An inter-columnar distance (a = 48.6 Å) was larger than that of **3C12BF4** as expected. Other VT-XRD patterns of fused π-conjugated imidazolium compounds are indicated as Fig. S43–45 in ESI†. Taking their POM images (Fig. S36–38 in †ESI) into consideration, only crystalline phases were corroborated for **3C8BF4**, **2C12BF4**, and **3C12TFSI**. It should be emphasized that the fused structure is quite essential to obtain a hexagonal columnar liquid crystal because **3C12BF4ref** only demonstrated a crystalline phase, as shown in Fig. S35 (DSC thermogram), Fig. S39 (POM image), and Fig. S46 (VT-XRD pattern) in ESI†.

Optical properties

Initially, UV-vis and fluorescence spectra were measured in CH_2Cl_2 solution. Fused π-conjugated imidazolium compounds bearing a trialkoxyphenyl group showed UV-vis spectra with the vibrational fine structure having peak maxima at 311 nm and 324 nm, which were independent of the alkoxy chain length and counter anion (Fig. S48 in ESI†, Left). They constantly emitted a fluorescence with a peak maxima at 409 nm, and relative quantum yields were around 0.55 (Table S3 in ESI†). On the other hand, a fused π-conjugated imidazolium compound bearing two dodecyloxy groups (**2C12BF4**) exhibited red-shift and blue-shift of UV-vis and fluorescence spectra, respectively, due to the electronic influence of the substituent (Fig. S48 in ESI†, Right). The fluorescence quantum yields were increased to be 0.78. UV-vis and fluorescence spectra of **3C12BF4** were also measured in THF and CH_3CN solutions. With increasing a solvent polarity, the emission peak maxima were slightly blue shifted and the highest fluorescence quantum yield (0.82) was obtained in CH_3CN solution. The increased fluorescence quantum yield can be ascribed to the diminished cation-anion interaction separated by solvent molecules and the suppression of non-radiative decay from the excited state (Fig. S49 in ESI†).[10]

Subsequently, optical properties were investigated in solid state. At the beginning, the spectra of **3C12BF4** were measured for an as-prepared sample and an annealed sample heated at 220 °C for 10 min. The UV-vis absorption spectrum showed a peak maximum at around 350 nm (Fig. S50 in ESI†).

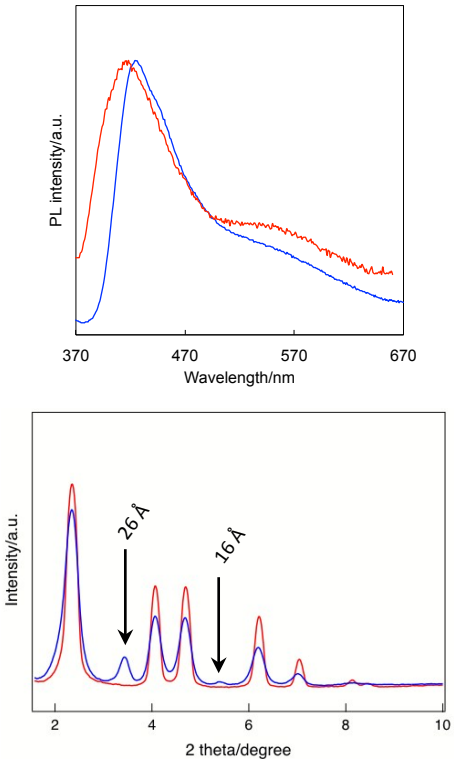

Fig. 8 Top: Fluorescence emission spectra of **3C12BF4** for (blue line) as-prepared sample and (red line) annealed sample obtained by irradiating at 350 nm. Bottom: XRD profiles of **3C12BF4** for (blue line) as-prepared sample and (red line) annealed sample.

The red-shift from solution state (325 nm) indicates the aggregated structure and chromophore interaction in the ground state. An as-prepared sample had a fluorescent peak maximum at 424 nm, by exciting at 350 nm, that exhibited a bathochromic shift from that in solution state (410 nm) (Fig. 8, Top, blue line). A shoulder peak was also observed at around 560 nm. A absolute fluorescence quantum yield (0.16) was lower than that in solution state (0.55). On the basis of XRD profiles, an as-prepared sample had diffraction peaks at ca. 26 Å and 16 Å in addition to peaks assignable to a hexagonal columnar phase (Fig. 8, Bottom). It can be considered that the metastable structure was included in an as-prepared sample. On the other hand, after the thermal annealing at the clearing temperature, the emission peak maximum (413 nm) showed a blue-shift and the longer wavelength shoulder became prominent (Fig. 8, Top, red line). Therefore a fluorescence spectrum of **3C12BF4** in the liquid crystalline phase could be an overlapped one of the aggregated and monomeric species. Fluorescence spectra were likewise measured for other two liquid crystalline compounds (**3C12OTf**, and **3C16BF4**) at room temperature after heating to the clearing temperature (Fig. 9). The emission peak maxima demonstrated a hypsochromic shift while the shoulder peak at around 560 nm became larger in the order of **3C12OTf**, **3C12BF4**, and **3C16BF4**.[14] Since this trend is in good agreement with the high and low regularity of

hexagonal columnar structures (*vide supra*, Fig. 5), the different fluorescence spectra between these compounds can be ascribed to the π-π interaction of fused π-conjugated systems. Namely, in the case of **3C16BF4**, the strong van der Waals and cation-anion interactions result in the marked chromophore interaction in the excited state. The fluorescence spectra of **3C12OTf** and **3C16BF4** were also measured upon excitation at 450 nm (Fig. S51 in ESI†). Although **3C12OTf** showed no detectable fluorescence, **3C16BF4** had an emission peak maximum at 565 nm implying the preferential excitation of the aggregated species.

For obtaining further insight into the fluorescence behavior, fluorescence lifetime measurements were conducted for **3C12BF4** in the liquid crystalline phase. Fig. 10 indicate the decay curves with the different excitation and monitor wavelengths. In all cases, the decay curves could be better fitted with a double-exponential function rather than a single-exponential one. This result suggests the presence of two radiative decay processes from the excited state. When **3C12BF4** was excited at 375 nm and monitored at 420 nm

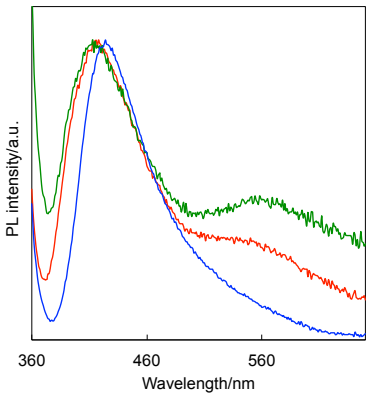

Fig. 9 Fluorescence emission spectra of (red line) **3C12BF4**, (blue line) **3C12OTf**, and (green line) **3C16BF4** in solid state obtained by irradiating at 350 nm.

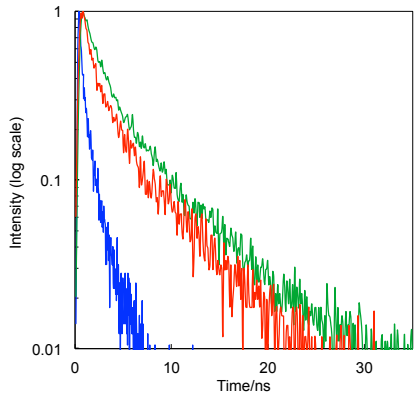

Fig. 10 Fluorescence decay curves of **3C12BF4**. Blue line: Excited at 375 nm and monitored at 420 nm. Green line: Excited at 375 nm and monitored at 550 nm. Red line: Excited at 425 nm and monitored at 550 nm.

(blue line), the fluorescence lifetime (τ) was calculated as 1.87 ns by the tail-fitting approximation. This value was shorter than that in CH_2Cl_2 solution (Fig. S52 in ESI†, τ = 2.21 ns) indicating the effective trap of excitation energy.[15] It was found from the figure, however, the decay curve excited at 375 nm and monitored at 550 nm (green line) was composed of τ = 6.76 ns. The longer lifetime is likely attributable to the excimer-like emission of fluorophores. On the other hand, a comparable lifetime (τ = 6.79 ns) was calculated when **3C12BF4** was excited at 425 nm and monitored at 550 nm (red line). This result would be also indicative of the selective excitation of aggregated fused π-conjugated imidazolium cations by the longer wavelength light (*vide supra*).

Conclusions

We have prepared a series of fused π-conjugated imidazolium compounds bearing two or three long alkoxy chains as well as a reference compound without the fused structure to investigate their self-organization and fluorescent properties. The phase transition behavior was largely influenced by both the alkoxy chain length and counter anion, and some compounds demonstrated an enantiotropic mesophase with a hexagonal columnar structure. The fused structure is quite essential to obtain a hexagonal columnar liquid crystal. Fused π-conjugated imidazolium compounds, particularly for that with the highly regular columnar structure, showed a longer wavelength emission in the liquid crystalline phase likely stemmed from the interaction of fluorophores. We believe that these results shed light on the design of smart functional materials interlinking self-organized nanostructures and optoelectronic properties.

Acknowledgements

A part of this work was conducted in Nagoya University, supported by Nanotechnology Platform Program (Molecule and Material Synthesis)of the Ministry of Education, Culture, Sports, Science and Technology (MEXT), Japan. Prof. Takuya Nakashima (NAIST) is also acknowledged for his helpful discussion about UV-vis and fluorescence spectra in solid state.

Notes and references

1 (a) S. Laschat, A. Baro, N. Steinke, F. Giesselmann, C. Hägele, G. Scalia, R. Judele, E. Kapatsina, S. Sauer, A. Schreivogel and M. Tosoni, *Angew. Chem. Int. Ed.*, 2007, **46**, 4832–4887; (b) S. Sergeyev, W. Pisula and Y. H. Geerts, *Chem. Soc. Rev.*, 2007, **36**, 1902–1929; (c) B. R. Kaafarani, *Chem. Mater.*, 2011, **23**, 378–396.

2 (a) N. Boden, R. J. Bushby, J. Clements and B. Movaghar, *J. Mater. Chem.*, 1999, **9**, 2081–2086; (b) L. Schmidt-Mende, A. Fechtenkötter, K. Müllen, E. Moons, R. H. Friend and J. D. MacKenzie, *Science*, 2001, **293**, 1119–1122; (c) A. M. van de

Craats, N. Stutzmann, O. Bunk, M. M. Nielsen, M. Watson, K. Müllen, H. D. Chanzy, H. Sirringhaus and R. H. Friend, *Adv. Mater.*, 2003, **15**, 495–499; (d) B. A. Gregg, *J. Phys. Chem. B*, 2003, **107**, 4688–4698; (e) C. D. Simpson, J. Wu, M. D. Watson and K. Müllen, *J. Mater. Chem.*, 2004, **14**, 494–504; (f) B. A. Jones, M. J. Ahrens, M.-H. Yoon, A. Facchetti, T. J. Marks and M. R. Wasielewski, *Angew. Chem. Int. Ed.*, 2004, **43**, 6363–6366; (g) W. Pisula, A. Menon, M. Stepputat, I. Lieberwirth, U. Kolb, A. Tracz, H. Sirringhaus, T. Pakula and K. Müllen, *Adv. Mater.*, 2005, **17**, 684–689; (h) Z. An, J. Yu, S. C. Jones, S. Barlow, S. Yoo, B. Domercq, P. Prins, L. D. A. Siebbeles, B. Kippelen and S. R. Marder, *Adv. Mater.*, 2005, **17**, 2580–2583; (i) H. Takezoe, K. Kishikawa and E. Gorecka, *J. Mater. Chem.*, 2006, **16**, 2412–2416; (j) D. Miyajima, F. Araoka, H. Takezoe, J. Kim, K. Kato, M. Takata and T. Aida, *Science*, 2012, **336**, 209–213.; (k) F. Araoka, S. Masuko, A. Kogure, D. Miyajima, T. Aida and H. Takezoe, *Adv. Mater.*, 2013, **25**, 4014–4017.

3 (a) C. J. Bowlas, D. W. Bruce and K. R. Seddon, *Chem. Commun.*, 1996, 1625–1626; C. M. Gordon, J. D. Holbrey, A. R. Kennedya and K. R. Seddon, *J. Mater. Chem.*, 1998, **8**, 2627–2636; (b) J. D. Holbrey and K. R. Seddon, *J. Chem. Soc., Dalton Trans.*, 1999, 2133–2139; (c) J.-M. Suisse, S. Bellemin-Laponnaz, L. Douce, A. Maisse-François and R. Welter, *Tetrahedon Lett.*, 2005, **46**, 4303–4305; (d) J. Y. Z. Chiou, J. N. Chen, J. S. Lei and I. J. B. Lin, *J. Mater. Chem.*, 2006, **16**, 2972–2977; (e) J.-M. Suisse, L. Douce, S. Bellemin-Laponnaz, A. Maisse-François, R. Welter, Y. Miyake and Y. Shimizu, *Eur. J. Inorg. Chem.*, 2007, 3899–3905; (f) K. Goossens, K. Lava, P. Nockemann, K. V. Hecke, L. V. Meervelt, K. Driesen, C. Görller-Walrand, K. Binnemans and T. Cardinaels, *Chem. Eur. J.*, 2009, **15**, 656–674; (g) M. Blesic, M. Swad´zba-Kwa´sny, J. D. Holbrey, J. N. C. Lopes, K. R. Seddon and L. P. N. Rebelo, *Phys. Chem. Chem. Phys.*, 2009, **11**, 4260–4268; (h) S. Kohmoto, Y. Hara and K. Kishikawa, *Tetrahedron Lett.*, 2010, **51**, 1508–1511.

4 (a) K. Hoshino, M. Yoshio, T. Mukai, K. Kishimoto, H. Ohno and T. Kato, *J. Polym. Sci. Part A: Polym. Chem.*, 2003, **41**, 3486–3492; (b) M. Yoshio, T. Mukai, H. Ohno and T. Kato, *J. Am. Chem. Soc.*, 2004, **126**, 994–995; (c) M. Yoshio, T. Kagata, K. Hoshino, T. Mukai, H. Ohno and T. Kato, *J. Am. Chem. Soc.*, 2006, **128**, 5570–5577; (d) H. Shimura, M. Yoshio, K. Hoshino, T. Mukai, H. Ohno and T. Kato, *J. Am. Chem. Soc.*, 2008, **130**, 1759–1765; (e) T. Kato, *Angew. Chem. Int. Ed.*, 2010, **49**, 7847–7848.

5 (a) W. Dobbs, L. Douce, L. Allouche, A. Louati, F. Malbosc and R. Welter, *New J. Chem.*, 2006, **30**, 528–532; (b) W. Dobbs, J.-M. Suisse, L. Douce and R. Welter, *Angew. Chem. Int. Ed.*, 2006, **45**, 4179–4182.

6 J. Motoyanagi, T. Fukushima and T. Aida, *Chem. Commun.*, 2005, 101–103.

7 B. E. Hamaoui, L. Zhi, W. Pisula, U. Kolb, J. Wu and K. Müllen, *Chem. Commun.*, 2007, 2384–2386.

8 (a) A. J. Boydston, C. S. Pecinovsky, S. T. Chao and C. W. Bielawski, *J. Am. Chem. Soc.*, 2007, **129**, 14550–14551; (b) A. J. Boydston, P. D. Vu, O. L. Dykhno, V. Chang, A. R. Wyatt, II, A. S. Stockett, E. T. Ritschdorf, J. B. Shear and C. W. Bielawski, *J. Am. Chem. Soc.*, 2008, **130**, 3143–3156; (c) K. M. Wiggins, R. L. Kerr, Z. Chen and C. W. Bielawski, *J. Mater. Chem.*, 2010, **10**, 5709–5714; (d) B. Dong, T. Sakurai, Y. Bando, S. Seki, K. Takaishi, M. Uchiyama, A. Muranaka and H. Maeda, *J. Am. Chem. Soc.*, 2013, **135**, 14797–14805.

9 (a) Y. Ren, W. H. Kan, M. A. Henderson, P. G. Bomben, C. P. Berlinguette, V. Thangadurai and T. Baumgartner, *J. Am. Chem. Soc.*, 2011, **133**, 17014–17026; (b) Y. Ren, W. H. Kan, V. Thangadurai and T. Baumgartner, *Angew. Chem. Int. Ed.*, 2011, **51**, 3964–3968.

10 K. Takagi, Y. Ito, K. Kusafuka and M. Sakaida, *Org. Biomol. Chem.*, 2013, **11**, 2245–2248.

11 K. Takagi, K. Kusafuka, Y. Ito, K. Yamauchi, K. Ito, R. Fukuda and M. Ehara, *J. Org. Chem.*, 2015, **80**, 7172–7183.

12 K. Binnemans, *Chem. Rev.*, 2005, **105**, 4148–4204.

13 A broad peak was also detected at 0.36 nm (2theta = 24.8 degree), which might be originated from the π-π stacking of fused π-conjugated imidazolium cations. See, T. Ogawa, M. Yoshida, H. Ohara, A. Kobayashi and M. Kato, *Chem. Commun.*, 2015, **51**, 13377–13380.

14 The absolute fluorescence quantum yields were 0.16, 0.04, and 0.05 for **3C12OTf**, **3C12BF4**, and **3C16BF4**, respectively.

15 A. Synak, B. Grobelna, L. Kułak, A. Lewkowicz and P. Bojarski, *J. Phys. Chem. C.* 2015, **119**, 14419–14426.